Synthesis of imprinted hydrogel microbeads by inverse Pickering emulsion to controlled release of adenosine 5'-monophosphate

Mohamed Ayari, Porkodi Kadhirvel, Patrick Favetta, Bernard Plano, Corinne Dejous, Benjamin Carbonnier, Luigi Agrofoglio

Synthesis of imprinted hydrogel microbeads by inverse Pickering emulsion to controlled release of adenosine 5'-monophosphate

Mohamed G. Ayari,[a,1] Porkodi Kadhirvel,[a,1] Patrick Favetta,[*,a] Bernard Plano,[b] Corinne Dejous,[b] Benjamin Carbonnier,[c] and Luigi A. Agrofoglio[*,a]

[a] *ICOA UMR CNRS 7311, Université d'Orléans, Rue de Chartres, 45067 Orléans, France*

[b] *IMS, Université de Bordeaux, CNRS UMR 5218, Bordeaux INP, 33405 Talence, France*

[c] *ICMPE, UMR CNRS 7182 - Université Paris Est, 2-8 rue Henri Dunant, 94320 Thiais, France*

* Corresponding authors. Tel: +33 238 494 582

E-mail addresses: patrick.favetta@univ-orleans.fr; luigi.agrofoglio@univ-orleans.fr

[1] Both authors have contributed equally to this work.

Abstract

Herein, we propose the synthesis of a microspherical imprinted hydrogel meant for the controlled release of a nucleotide, adenosine 5'-monophosphate (5'-AMP). Indeed, molecularly imprinted polymers-based (MIPs) materials possess remarkable selective molecular recognition ability that mimicks biological systems. MIPs have been used in numerous applications and hold great promise for the vectorization and/or controlled release of therapeutics and cosmetics. But, the conception of imprinted hydrogels-based drug delivery systems that are able to release polar bioactive compounds is explored weakly. Herein, the synthesis of imprinted hydrogel microbeads by inverse Pickering emulsion is detailed. Microspheres showed a large 5'-AMP loading capacity, around 300 $mg.g^{-1}$, and a high binding capacity comparatively to the non-imprinted counterpart. The MIP had a thermo-responsive release behaviour providing sustained release of adenosine 5'-monophosphate in an aqueous buffer simulating both human skin pH and temperature.

Keywords: Molecularly imprinted microparticles, Adenosine 5'-monophosphate, bioactive release, inverse Pickering emulsion, hydrogel microspheres, skin anti-ageing

1. Introduction

Molecular imprinting technology is applied in the preparation of polymers which have selective molecular recognition properties for a given target compound [1]. A polymer network is formed by co-polymerization of the functional monomer and cross-linker, around a template molecule, creating memory cavities [2-7]. The generated cavities are complementary in size, shape and functionality to the template, and can recognize the targeted compound with high selectivity. Based on this remarkable behavior of molecular recognition, MIPs are also named synthetic receptors [8], synthetic enzymes [9] or synthetic antibodies [10], and they can be employed to wide range of applications, such as analytical separation, immunosorbent assay, sensing, etc. [11].

More recently, imprinted polymers have emerged as powerful and versatile drug delivery system (DDS) taking advantage of their intrinsic properties such as high affinity binding cavities, minimized burst effect, optimized dosing and triggered release [12, 13]. Despite a growing number of publications in the field of MIP- based DDS [14], only a few works have focused on cosmetics delivery. For instance, MIP hydrogel film were applied to release of hyaluronic acid at a controlled rate [15].

The aim of this work is to synthesize a water-compatible MIP, as hydrogel microspheres, selective to 5'-AMP and allowing for its release in topical conditions. Because of age-related alteration of skin functions including protection and regulation, wound repair and regeneration are vital to maintain organisms protection from their environment and can be effectively achieved via the topical releasing of bioactives [16]. Antioxidant topical agents

such as vitamins or polyphenols, were primarily used against human skin aging phenomenon [17]. It has been suggested recently that 5'-adenosine monophosphate (5'-AMP) accelerates the human epidermal turnover that is related to the energy metabolism of epidermal basal cells and typically delayed by aging. This 5'-AMP-mediated beneficial effect can be rationalized by the fact that 5'-AMP increases the amount of intracellular 5'-adenosine triphosphate (5'-ATP), which is needed for cell renewal and division [18].

Although various synthesis strategies have been explored relying on either specifically designed monomer-solvent combinations [19] or the conventional poly(methacrylic acid-*co*- ethyleneglycol dimethacrylate)-based MIP [20] to prepare MIP exhibiting high binding capacity in physiologically-relevant conditions, current technology often fails to generate MIPs for use in pure aqueous environments. As suggested by Kanekiyo *et al*. working on the recognition of 5'-AMP, an elegant approach relies on the use of a mixture of polymers with oppocavity charge, such as poly(diallyldimethylammonium) and polyboronate, without cross-linking, to form a "footprint" of the bioactive target. Both capture and release of 5'-AMP were correlated to the precipitation and swelling of the polyions' complex [21]. The polyion complex formation approach has been extended to the preparation of quartz crystal microbalance resonator systems for 5'-AMP sensing [22, 23]. However, to the best of our knowledge, it has not yet been successfully applied as drug delivery systems. Other studies reported on the incorporation of a hydrophilic co-monomer as 2-hydroxyethyl methacrylate in the MIP formulation [24] or, as demonstrated more recently by Ye *et al.*, the implementation of a new polymerization technique, namely inverse Pickering emulsion polymerization route, in order to prepare water-compatible MIPs directly in water [25]. This latter approach allowed the molecular imprinting of very polar templates, that are soluble almost exclusively in water, such as proteins [26] or nucleotides, such as 5'-AMP, as will be shown in this study. The key step is to obtain a stable pre-polymerization

complex, as water may disrupt the interactions between template and monomer(s) molecules through competitive hydrogen bonding. So, based on previous studies, 2-(dimethylamino)ethyl methacrylate (DMAEM) and N-isopropylacrylamide have been judiciously selected as monomers providing ionic interactions with anionic phosphate moiety of 5'-AMP [27], and hydrogen bonding, even in water, with the nucleobase and the ribose moiety, [28, 29] respectively. It is worth mentioning that hydrophobic interactions may also be involved. In this contribution, inverse Pickering emulsion polymerization was successfully applied to the preparation monodisperse hydrogel microbeads incorporating molecularly imprinted binding cavities towards 5'-AMP in water based on an optimal combination of hydrophobic, hydrogen bonding and electrostatic interactions. The potential of the so-designed MIP microbeads for the sustained release of 5'-AMP in biological medium mimicking the skin pH and temperature is investigated.

2. Experimental

2.1 Materials

Adenosine-5'-monophosphoric acid (99%, 5'-AMP) was purchased from Thermo Fisher, Karlsruhe, Deutschland. N-isopropylacrylamide (>98.0%, NIPAM) was procured from TCI Europe NV, Zwijndrecht, Belgium. Hydroxylamine solution (50 wt.% in H_2O, 99.999%), *N,N'*-Methylenebis(acrylamide) (99%, MBAM), 2-(dimethylamino)ethyl methacrylate (98%, DMAEM), silica nanopowder (spec. surface area 175-225 m^2/g, 99.8%, 12 nm diameter), trimethylsilyl chloride (≥ 99%, TMSCl), toluene (HPLC grade ≥ 99.9%) and hydrofluoric acid 48 wt. % in H_2O (≥99.99%, HF) were bought from Sigma Aldrich, St. Quentin Fallavier, France. 1,2-Bis(2-(4,5-dihydro-1H-imidazol-2-yl)propan-2-yl)diazene dihydrochloride (95%, VA-044) was obtained from Fluorochem, Hadfield, United-Kingdom.

Ultra-High-Quality water (18 MΩ.cm) was produced from an Elga apparatus, Villeurbanne, France.

2.2 Silica nanoparticles derivatization

For successful inverse Pickering emulsion polymerization, the dried silica nanoparticles were derivatized in order to make them hydrophobic. The optimized weight ratio nanoparticles / derivatization agent was found to be 10/1 [30]. For this, in a 100 ml flask, 3 g of silica nanoparticles were added to 30 ml of toluene with continuous stirring to obtain homogeneous suspension. Then 0.3 g of TMSCl was added slowly to this suspension. It was left stirring for 15 min at room temperature. After, the solvent was allowed to evaporate overnight to obtain dry nanoparticles. Silica nanoparticles were then stored under an argon atmosphere in a dry environment.

2.3 Synthesis of 5'-AMP MIP and NIP by inverse Pickering emulsion polymerization

The formulations for the preparation of microspheres are summarized in Table S1, in the supplementary data. 30 mg of derivatized silica nanoparticles and 10 g of toluene were mixed in a 20 mL clear vial and sonicated for 5 min to form a homogeneous suspension. Subsequently, the aqueous solution containing 5'-AMP (405 mg), DMAEM (167 mg), NIPAM (528mg), MBAM (89mg), 2.8 g of water and water-soluble initiator VA-044 (2 mg), was added in the oil phase, the mixture was sonicated for 2 min and emulsified with a vortex mixer at 3000 rpm for 3 min to obtain a stable inverse suspension. This aqueous solution was de-oxygenated by bubbling N_2 at room temperature for 10 min before mixing. The emulsion droplets obtained are visualized by optical micrography to confirm the successful formation of the emulsions (Fig. S2) [31]. The emulsion is polymerized in a UV oven overnight to obtain hydrogel microspheres. After filtration, the beads were washed with methanol three times and dried at 50°C under vacuum for 12 h to remove water and toluene. In order to

remove hydrophobic silica nanoparticles on the surface of MIP or NIP, the hydrogels were placed in 15 mL polyethylene centrifuge tubes containing 24% HF aqueous solution and vibrated for 48h at ambient temperature in a ThermoMixer C (Eppendorf, Dutscher, Brumath, France), . The total dissolution of the silica nanoparticles was evidence by FTIR, based on the intensity of the stretching band of the Si-O bond at 1076 cm^{-1}, as shown in Figure S3. Later on, MIP microspheres were washed several times with high-purity water to eliminate HF, until pH of the washing solution becomes close to water pH. Then, the template was extracted with the same volumes of a MeOH/$NH_{3(aq)}$ pH 10 (50/50, v/v) solution, under sonication during 30 min. The pH was adjusted to 10 units providing deprotonation of the amine function of DMAEM (pKa = 8.42) and thus enabling disruption of the electrostatic bonds between the MIP and the template. The extraction procedure of the template was completed when the absorbance measured at the maximum wavelength of the 5'-AMP in the washing solution (262 nm) was practically equal to zero. Following, the polymeric particles were washed with methanol and placed in a vacuum heated desiccator. Correspondingly, non-imprinted polymers (NIP) were prepared following the same steps of MIP preparation omitting the addition of template. Scheme 1 shows schematic illustration of the preparation route of 5'-AMP-imprinted hydrogel microparticles.

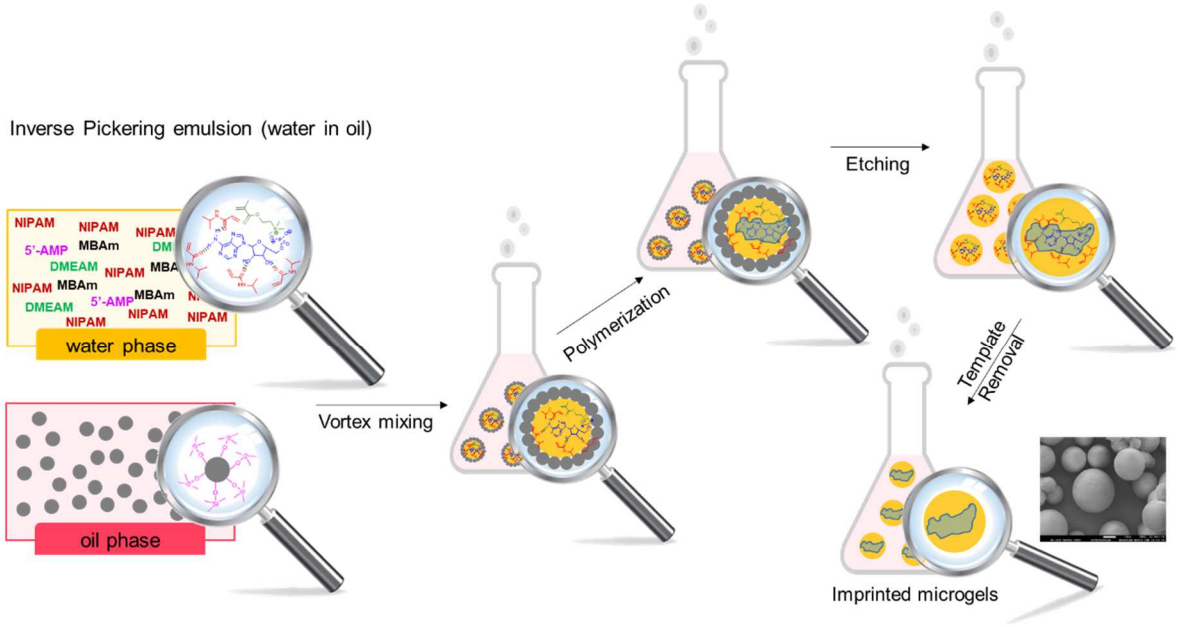

Scheme 1. Scheme of preparation of inverse Pickering emulsion to synthesize MIP-DMEAM-NIPAM-based hydrogel microbeads.

2.4 Scanning Electron Microscopy (SEM) Analysis

The morphology of samples was observed using a field emission scanning electron microscopy (FEG, JEOL JSM 7800F Prime), Ultra high resolution (optimal magnification: 1.000.0000, Resolution: 7 Å from 30kV to 1 kV). Observation conditions were as follows: work distance: between 6mm and 10mm, Accelerating voltage: 1 kV to 5 kV, large Depth of Focus (LDF) mode. Polarized support 5kV (super-high resolution Gentle Beam (GBSH)) + scanning CF (Charge Free). Pre-treatment of samples: powders were depocavited on self-adhesive carbon pellets then a gold film was depocavityd with a thickness of about 5nm by cathodic sputtering on the whole support prior to SEM observation. To complete analysis, a second device is used: a LEO Gemini 1530 SEM apparatus (Leo Elektronenmikroskopie, Oberkochen, Germany). Prior to scanning electron microscopy (SEM) analysis the polymer

samples were depocavited onto SEM supports with a silver-containing solution, dried under reduced pressure and further coated with a thin platinum layer (2 nm) using a sputter coater Cressington 208 HR (Elektronen Optik Service, Dortmund, Germany). SEM analysis was performed using scanning electron microscopy with the help of a LEO Gemini 1530 SEM apparatus (Leo Elektronenmikroskopie, Oberkochen, Germany).

2.5 FT-IR analysis

Fourier Transform Infrared Spectrometer, scan range: MIR 3900–650 cm^{-1}, resolution 1.0 cm^{-1}, and 64 as number of scans. The Shimadzu - MIRacle 10 (IRaffinty 1), is equipped with Ge Cristal and is driven by IRsolution 1.50 software.

2.6 Swelling measurement

In order to better elucidate the difference between the dry and swollen states of the MIP polymers, swelling tests were performed in water. Swelling measurements were made by gravimetric measurement. A known weight of dry hydrogel sample (around 10 mg) was measured in an eppendorf tube and suspended in 1 mL of pure water at 25°C. After 24 h, the hydrogel sample was recovered, quickly blotted free of surface water using filter paper and weighed on an analytical balance (reproducibility 0.03 mg). The swelling ratio was calculated using the equation (1):

$$\text{Swelling ratio} = (\text{swollen sample weight} - \text{dry sample weight}) / \text{dry sample weight} \quad (1)$$

2.7 Quantification of loading capacity.

For spherical materials, the adsorption isotherms were determined using batch method. For this, 20 mg of each MIP and NIP polymer particles were placed in 1.5 mL

Eppendorf tubes, and 1 mL of aqueous hydroxylammonium acetate 1mM, pH = 7, solution with different concentrations of 5'-AMP was added. Each suspension was gently shaken for 16 h at 25°C in ThermoMixer C, and the supernatants were separated by centrifugation. The concentration of 5'-AMP in the supernatant solutions was measured by HPLC. The amount of 5'-AMP adsorbed at equilibrium (B, $mol.g^{-1}$) was calculated according to Eq (2): [32]

$$B = \frac{V \times (C_0 - F)}{m} \quad (2)$$

where C_0 and F are the initial and equilibrium concentrations of 5'-AMP in solution ($mol.L^{-1}$), respectively, V (L) is the volume of the solution, and m (g) is the weight of the polymers.

All aqueous solutions of 5'-AMP were analysed in an Agilent 1260 Infinity HPLC chromatograph (Agilent Technologies, Les Ulis, France). The chromatograph was equipped with a 1260 binary pump (G1311B), a 1260 standard autosampler (G1329B), a 1260 thermostated column compartment (G1316A) and a 1260 diode array detector (G4212B) with a Max-Light cartridge cell (1 µL volume, 10 mm cell path length). A silica grafted C18 HPLC column (Prevail® C18, 150 mm × 3 mm i.d., 5 µm particle size) (Grace, Epernon, France) was used. The injection volume was 5 µL. The temperature of the oven was set at 30 °C. The separation of analytes was performed using isocratic elution with ammonium acetate 25mM pH = 7 aqueous solution/acetonitrile (95/5, v/v) with a flow rate of 0.4 mL/min. 5'-AMP was quantified at 260 nm.

2.8 Kinetic study of 5'-AMP release

Hydrogel beads obtained from inverse Pickering emulsion polymerization (50 mg) were soaked in 1.5 mL of 5'-AMP aqueous hydroxylammonium acetate solution (1 mM) pH = 7, at 28.8 mM. After 24 h, the suspension was centrifuged at 5000 rpm for 5 min and the microparticles were recovered and further dried at 40°C overnight in a vacuum heated

desiccator. 5'-AMP concentration in the supernatant was quantified using the HPLC method and the mass of 5'-AMP loaded in the polymer particles was determined. The same procedure was performed for NIP hydrogels. The kinetic study of 5'-AMP release from MIP and NIP hydrogel microbeads was conducted by placing 50 mg of each 5'-AMP-loaded material in a 50 mL flask containing 40 mL of aqueous lactic acid solution, 5 mM, pH = 5.5, to mimic the skin pH. The suspension was gently stirred with a magnetic bar. In this kinetic study, the 5'-AMP concentration was measured by collecting 200 µL of solution at varied times. The collected solution was filtrated prior to injection in the HPLC.

3. Results and discussion

3.1 Choice of monomers, solvent and crosslinker

The successful preparation of hydrogel microspheres by polymerization based on reverse Pickering emulsion requires the use of water-soluble template, monomers, cross-linker and initiator. 5'-AMP is naturally soluble in water, and the monomers have been chosen accordingly. DMAEM, a basic monomer, has been previously studied in the laboratory to demonstrate its ability to interact with the phosphate group of nucleotide in DMSO or water through solid-phase extraction method [27]. Moreover, its toxicity, once polymerized, is very low [33]. However, in reverse Pickering emulsion, the two solvents mustn't be miscible. So that DMSO couldn't be selected as polar solvent to form droplets in an organic continuous phase. Indeed, DMSO is miscible in apolar solvent as toluene or partially soluble in hexane or cyclohexane, being the organic solvents usually used in inverse Pickering emulsion. DMSO was then replaced by the non-toxic solvent water and the MIP were synthetized as hydrogels. Furthermore, in water at neutral pH, DMEAM is under its cationic form because the amine group of is protonated (pKa of amine group is 8.42) and forms ionic interactions with the acid moiety of 5'-AMP (pKa are 1.22 and 6.27 for the both

hydroxyls of phosphate function) [34]. Besides, the 1:1 stoichiometry of 5'-AMP:DMEAM complex is demonstrated by a job plot obtained by UV spectrophotometry (Fig. S1). In order to enhance recognition of 5'-AMP, a second monomer containing an amide functional group is added in the MIP formulation. This type of monomer has been proved in a previous study to allow the formation of cavities selective towards the purine moiety of 5'-AMP *via* non-covalent interactions in DMSO solvent [27]. But here, in order to provide thermo-sensitive property to the MIP, acrylamide has been changed by NIPAM which forms polymer exhibiting a lower critical solution temperature (LCST) in water, close to body temperature. Furthermore, poly(NIPAM) is not cytotoxic to fibroblast cell type in direct contact tests [35] and its incorporation together with DMEAM within copolymer chains reduces cellular toxicity [36]. To determine the number of NIPAM equivalents to be added to the MIP formulation, a job plot method applied to the complex (5'-AMP-DMEAM):NIPAM in water (Fig. S1). The stoichiometry is found to be 1:4, suggesting that there is 1 (5'-AMP:DMEAM) complex for 4 NIPAM monomers. *N,N'*-Methylenebisacrylamide is chosen as cross-linker because of its large solubility in water (soluble 20 g/L at 20°C) and its use in biomedical applications [37]. The initiator selected is a water-soluble azo initiator, which has a ten-hour half-life decomposition temperature of 44°C and a good photoreactivity [38]. The polymers synthesized from inverse Pickering method are named SHMIP and SHNIP, with SH as spherical hydrogel.

3.2 Characterization of chemically modified silica nanoparticles

The ATR-FTIR spectra of silica particles as obtained before and after chemical modification with TMSCl are shown in Fig. 1. Compared to the non-derivatized SiO_2, the TMSCl-modified nanoparticles displayed no hydroxyl absorption band around 3400 cm^{-1}. New absorption bands around 2980 cm^{-1} corresponding to CH_3 stretching appeared. These

FTIR results suggest that the surface modification of SiO_2 nanoparticles with TMSCl was effective. The different surface properties of native SiO_2 and hydrophobic SiO_2 nanoparticles were monitored by adding said nanoparticles in a vial containing a toluene /water mixture. The hydrophilic nanoparticles remained in suspension in water, while the hydrophobic ones were transferred into the toluene phase, as shown in Fig. 1.

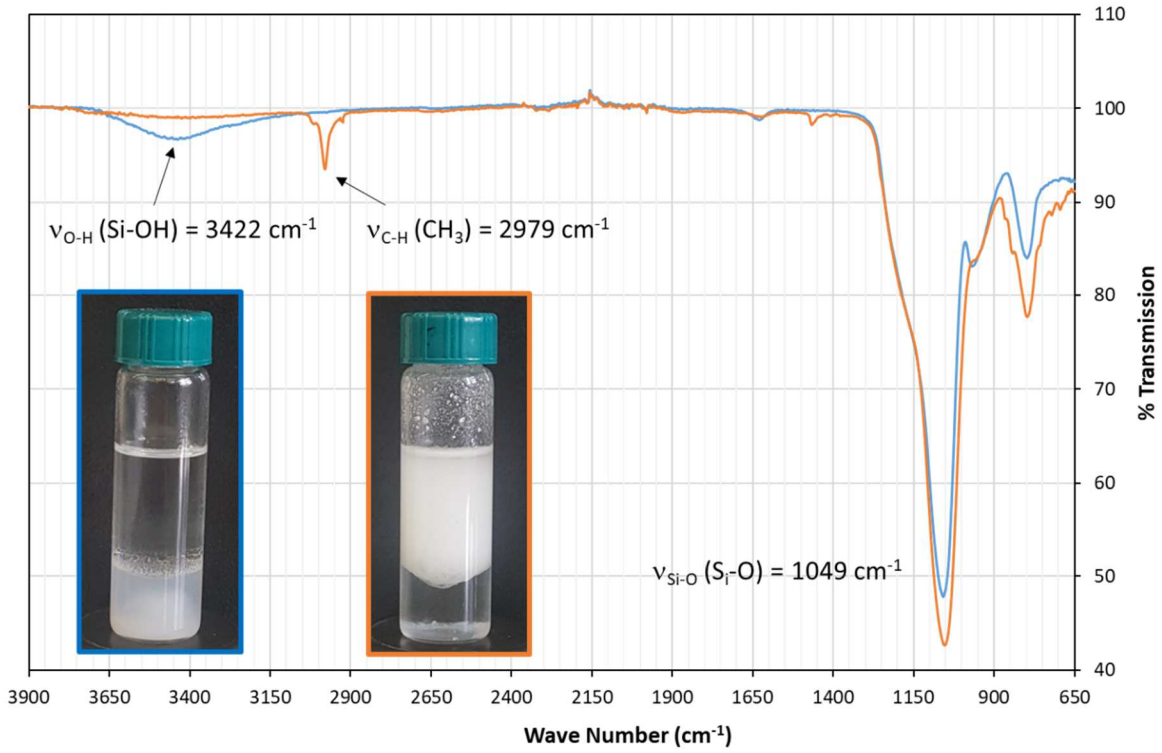

Fig. 1. FTIR spectra of bare silica nanoparticles (blue line) and hydrophobic ones (orange line), and results showing a suspension of polar unmodified and hydrophobized SiO_2 particles in a water / toluene mixture are showed. The unmodified SiO_2 are dispersed in water (lower layer, blue framed), while the apolar nanoparticles are dispersed only in toluene (upper layer, orange framed).

3.3 Inverse Pickering emulsion polymerization

The Pickering emulsion polymerization possesses many advantages over classical emulsion polymerization, because the non-use of surfactant reduces foaming problems,

induces lower toxicity and lower costs [39]. Pickering reverse emulsion technique is used to produce hydrogel spherical particles. Herein, surface modified silica nanoparticles are used to stabilize the emulsion. As demonstrated by Finkle *et al.*, the phase that preferentially wets the solid particles constitutes the continuous phase [40], here, the oil phase. Based on the work by Binks *et al.*, we have chosen to use silica nanoparticles with a diameter between 10 and 30 nm and treated with chlorotrimethylsilane, providing water-in-oil emulsions [41]. In the preparation of both imprinted or non-imprinted hydrogel beads, two different phases were prepared separately. Water phase containing the two monomers, crosslinker, template and initiator, and oil phase constituted of toluene containing hydrophobic silica nanoparticles. The toluene is taken as oil phase, because aromatic oils prefer w/o emulsions, whereas that non-polar oils such as alkanes and cycloalkanes prefer o/w emulsions [40]. In addition, toluene shows very low changes in the droplets size distribution in time, as compared to other aromatic alkenes. So, with toluene, the Ostwald ripening is minimized [42]. The photopolymerization technique is opted comparatively to thermo-driven polymerization, because Pickering emulsions can show a low thermal stability, and that could be a critical issue during thermal polymerization process [43]. Also, it was shown in literature that photo-initiated polymerization occurring at low temperature allows decreasing the kinetic energy of the prepolymerization complex and thus increasing its stability. Greater binding capacity and selectivity are thus obtained through photopolymerization as compared to thermally initiated polymerization which requires, in most cases, temperatures higher than 40°C [44-46]. The mass ratio between the oil phase and hydrophobic nanoparticles is very important. Here, the mass of silica nanoparticles is 30 mg for 10 g of toluene, as inspired by a previously published study on the synthesis of poly(*N-iso*propylacrylamide) beads by reverse Pickering emulsion [29]. The concentration of the nanoparticle must be optimized to entirely securing the droplet surface to cover entirely the water-oil interface, and avoid droplet ripening and

flocculation. The mass ratio between dispersed phase (aqueous phase) and continuous phase (toluene) is calculated to be 0.4 (with a volume ratio of 0.32) [25].

3.4 Morphology and particles size of the imprinted polymers

Scanning electron microscopy (SEM) is employed to determine the shape and surface morphology of the polymer particles produced using optimized formulation. The image from SEM showed that SHMIP and SHNIP particles are spherical with rough surface showing a mean diameter of 24 µm, with a size in the range between 10 and 50 µm (Fig. 2).

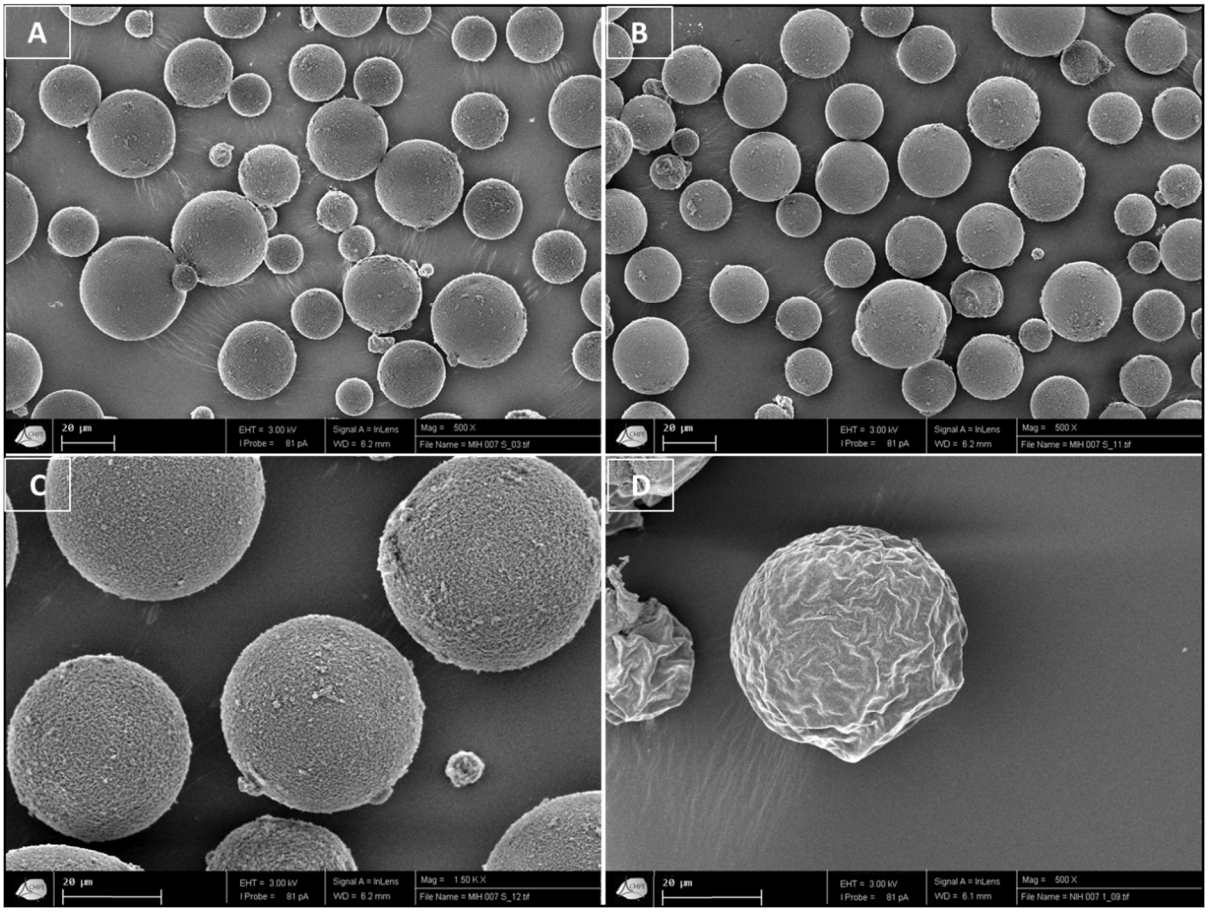

Fig. 2. SEM images of SHMIP (A) and SHNIP (B) microspheres. SHMIP (C) as prepared by inverse Pickering emulsion polymerization before HF etching and SHMIP as observed (D) after HF etching. Scale bar was 20 µm for all pictures.

3.5 Characterization of hydrogels

The characterization of affinity and capacity of the synthesized polymers for the 5'-AMP is performed by batch method for SHMIP and SHNIP. Adsorption isotherms provide important information concerning binding energies and number of cavities in the imprinted materials. During the binding process, molecules of template present in the solution are interacting with recognition cavities on MIP or with the non-specific cavities on NIP. Adsorption isotherms of SHMIP/SHNIP are shown in Fig. 3, by plotting template concentrations bound in materials (bound concentration B) according to template concentrations in solution (free concentration F), under constant temperature, 25°C, at equilibrium. Both isotherms present an S-shape, or sigmoidal type, in the concentration domains used. When an overall isotherm fits an S-shape, the observed "nonideality" comes from surface heterogeneity of polymers, with adsorbate-adsorbent phenomenon, or from a cooperative process due to lateral interactions between adsorbates. But, each phenomenon requires the use of two distinct isotherm models in order to extract the different parameters characteristic of the polymers. First, the combined Langmuir-Freundlich model (LF) could be used because it usually describes adsorption of a monolayer of template to a heterogeneous surface as found in molecularly imprinted surfaces [47]. The other equation describing adsorption of molecules involving a cooperative process on a homogeneous surface is the Hill model (H). However, both equations are mathematically equivalent (equation (3)) [48]. The mathematical forms of the Hill and the Langmuir-Freundlich equations are identical, only the values of power term '*m*' are different. In LF model, *m* is named heterogeneity parameter and values must be comprised between 0 and 1, the closer to 1 the value is, the more heterogeneous is the surface. In Hill model, *m* is the Hill coefficient and when $m = 1$ this indicates a non-cooperative system (Langmuir model), when $m > 1$ this indicates positive cooperativity (adsorption becomes easier when the coverage increases), and when $m < 1$ this

indicates negative cooperativity heterogeneity (adsorption becomes more difficult when the coverage increases). Hill model is already used for the characterization of MIPs [48]. The equation used in this work was:

$$B = \frac{B_{max} \times K^m \times F^m}{1 + K^m \times F^m} \quad (3)$$

B is the concentration of template bound to the MIP or NIP (mol.g^{-1}), B_{max} is the maximum adsorbed quantity (mol.g^{-1}), *m* is the Hill parameter, *K* is association constant (L.mol^{-1}), and F is the free template concentration in the solution after equilibrium (mol.L^{-1}). The experimental data from batch experiments are plotted on Fig. 3, where *B* and *F* are given in µmol.g^{-1} and µmol.L^{-1}, respectively, for an easier reading. The adsorption isotherm parameters are determined by non–linear regression with Origin Pro 2017, and the recovery between experimental and calculated data was evaluated by calculation of the values of reduced chi square χ^2, the coefficient of determination r^2 and the Fisher test value [50]. The models of Freundlich (F) and Langmuir (L) are applied to our experimental values, to compare the most used models in adsorption isotherms to the retained model. Hill results are showed in Table 1, while F and L data are listed in Table S2. The first information was that all *m* values were greater than 1, supposing that the adsorption phenomenon involved relied on positive cooperativity. For SHMIP, the value of *m* is very close to unity, which would suggest that the adsorption on its surface could follow the Langmuir theory, where adsorption would take place at selective homogeneous cavities within the adsorbent, with one template molecule occupying one imprinted cavity; the holy grail of any researcher on MIPs [51]. The fact to have $m > 1$, suggested probably, that more than one 5'-AMP molecule occupied one type of cavity. Probably, one 5'-AMP is first bound by electrostatic interactions to the cavity (or *via* non-specific interactions on the surface) while association of a second adsorbed 5'-AMP could be caused by π stacking interactions with nucleotide bases of the firstly present

molecule. This phenomenon could be accentuated by the swelling of polymers occurring in aqueous medium. Aggregates formation took place on the surface and so the Hill parameter could be presented as the number of molecules present in one binding cavity [49,52]. Despite this mathematical fact, when the Hill model is applied in our practical situation, the cooperativity parameter might therefore be affected by cavity heterogeneity, because imprinted material is very known to show heterogeneous distribution of binding cavity affinities, and it is very difficult to discriminate heterogeneity and cooperativity parts contained in the *m* value. But, the adsorption behavior of 5'-AMP on imprinted and non-imprinted polymers was determined by the same model, so it was easier to compare their B_{max} and *K* parameters. In terms of capacity, the equivalent number of 5'-AMP by mass unity, or B_{max}, was larger for MIP than for the corresponding NIP. However, to evaluate the real performance of MIP, the amount of template that can be selectively bound to the imprinted matrix versus the contribution of the non-specific binding, or ratio B_{max}(MIP) on B_{max}(NIP) for the same F of 5'-AMP, namely the imprinting factor (IF), has been calculated. Results showed imprinting factor equal to 3 at saturation concentration of 5'-AMP in solution, here taken to 15000 $\mu g.mL^{-1}$. The calculated IF value is similar to that obtained in the recent literature on drug release by MIPs [53]. This further supported the conclusion that the synthesis of polymers by inverse Pickering emulsion was an effective method to create imprinted hydrogel microbeads. The binding capacity is related to the porosity of the material and, hence, to the specific surface area of MIP. With a hydrogel, it is very difficult to obtain such parameters, so investigation of the swelling property is commonly performed. At room temperature, we have measured swelling ratio of 12.3 and 14.9 for SHMIP and SHNIP, and these results were in agreement with those found in the literature for poly(NIPAM) type hydrogels [52]. The swelling degree in aqueous solution was important for both polymers, but this behavior could not explain the binding capacity calculated for both MIP/NIP couples

because the swelling ratio were practically identical for SHMIP versus SHNIP. The larger capacity of SHMIP could not be correlated only to its swelling degree in aqueous solution. So, to evaluate the potential of using MIP hydrogels in drug delivery applications, the large capacity of the SHMIP is a very interesting parameter. Moreover, the drug template should be released under mild conditions, such as physiological conditions, and binding to polymer has to be reversible. As the binding affinity reflects the binding strength between the template and the complementary binding cavity in the MIP, it was important to compare the equilibrium binding constant *K* presented in the Table 1. For this parameter the spherical imprinted hydrogel was found to show the highest value. This value was the mean of all binding constant of 5'-AMP toward various types of adsorption cavities on heterogeneous polymer surface. Nevertheless, as the range of concentration where the *K* value was measured was the same for both polymers, we concluded that the SHMIP showed a better affinity for 5'-AMP molecule. The high *K* value calculated for SHMIP suggests a possible controlled release of 5'-AMP, because the value was high enough to retain the bioactive molecule in MIP cavities and prevent complete burst, and low enough to allow at the same the release of the bioactive molecule from the MIP cavities once in contact with the physiological medium.

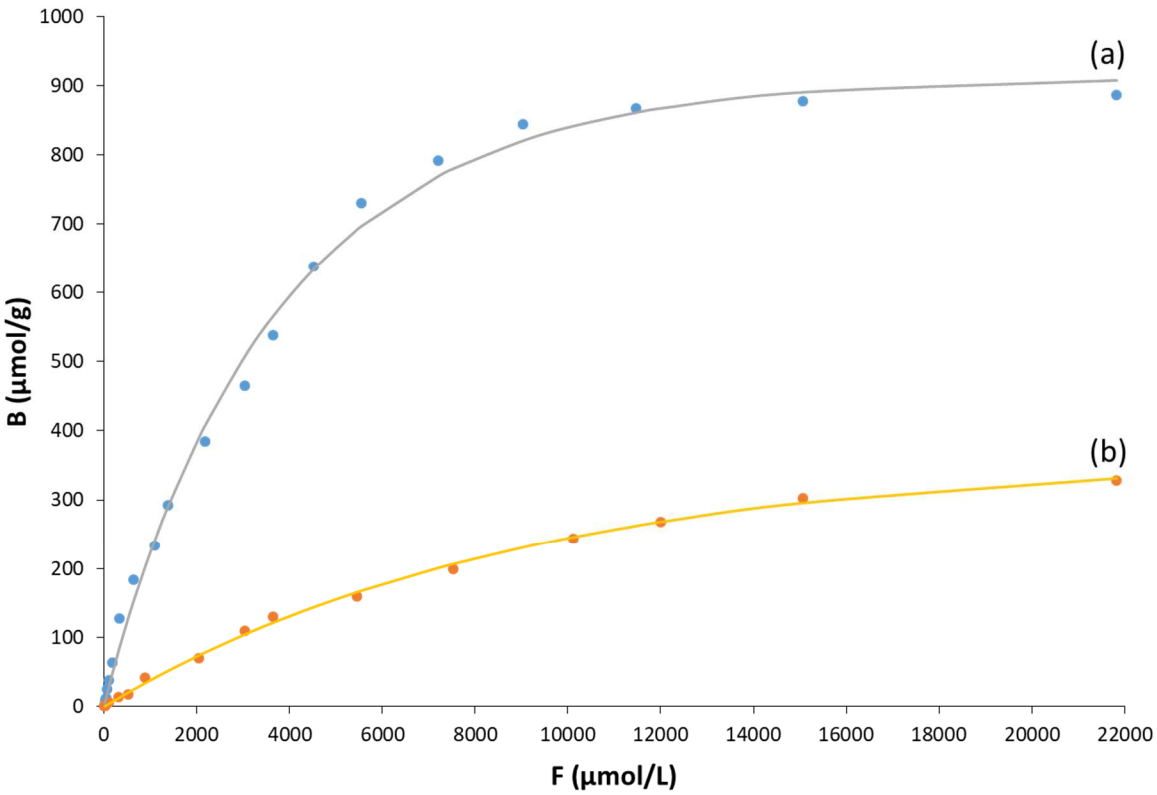

Fig. 3. Comparison between experimental adsorption data of 5'-AMP and values calculated using the Hill model. Free template concentration was between 11 to 21830 µmol.L^{-1}. Blue points represent B values measured for SHMIP and Orange points represent B values for SHNIP. Curves (a) and (b) are based on theoretical values obtained by Hill model for SHMIP and SHNIP, respectively.

Table 1. Batch results for SHMIP and corresponding SHNIP as affinity constants (K, L.mol^{-1}), number of binding cavities (B_{max}, mol.g^{-1}), coefficient of determination (r^2), the reduced chi square value (χ^2) and the statistical value of the Fisher test (F-test).

Model	Parameters	SHMIP	SHNIP
Hill	$\mathbf{B_{max}}$ (mol.g^{-1})	(10.61±1.58)×10^{-4}	(2.25±0.37) ×10^{-4}
	K (L.mol^{-1})	275.4±12.5	53.2±4.2
	m	1.052±0.027	1.342±0.036

r^2	0.99929	0.99951
χ^2	9.27×10^{-11}	2.99×10^{-12}
F-test	20080	19678

3.6. Kinetic study of 5'-AMP release

The spherical shape of MIP offered the advantage of eliminating the anisotropic swelling associated with other geometries and thus allowed improved control over the drug delivery process [54]. So, the kinetics of release are measured for SHMIP and compared to its reference, SHNIP. Before studying 5'-AMP release as a function of time and temperature, 50 mg of each polymers synthesized by inverse Pickering emulsion are loaded into a concentrated aqueous template solution (28.8 mM) for 24 hours. Amounts of 5'-AMP loaded on the polymers were quantified and the results were 316.05 $mg.g^{-1}$ (9.10×10^{-4} $mol.g^{-1}$) for SHMIP and 66.03 $mg.g^{-1}$ for SHNIP (1.90×10^{-4} $mol.g^{-1}$). These concentrations of template bound to polymers were very close to saturation concentrations found theoretically from the adsorption isotherm model, named B_{max}, 10.61×10^{-4} $mol.g^{-1}$ and 2.25×10^{-4} $mol.g^{-1}$ for SHMIP and SHNIP, respectively. The release study of 5'-AMP from SHMIP and SHNIP, in a simulated skin environment was also investigated. Indeed, according to literature, the skin has an average acidic pH of 5 and a temperature of 35°C [55]. To carry out this simulation, we chose to work with an aqueous solution of lactic acid at 5 mM, pH = 5.5, and at two temperatures, 25°C and 35°C. The release profiles are shown on Fig. 4. The release measurements are repeated 3 times for each formulation at each temperature (n = 3).

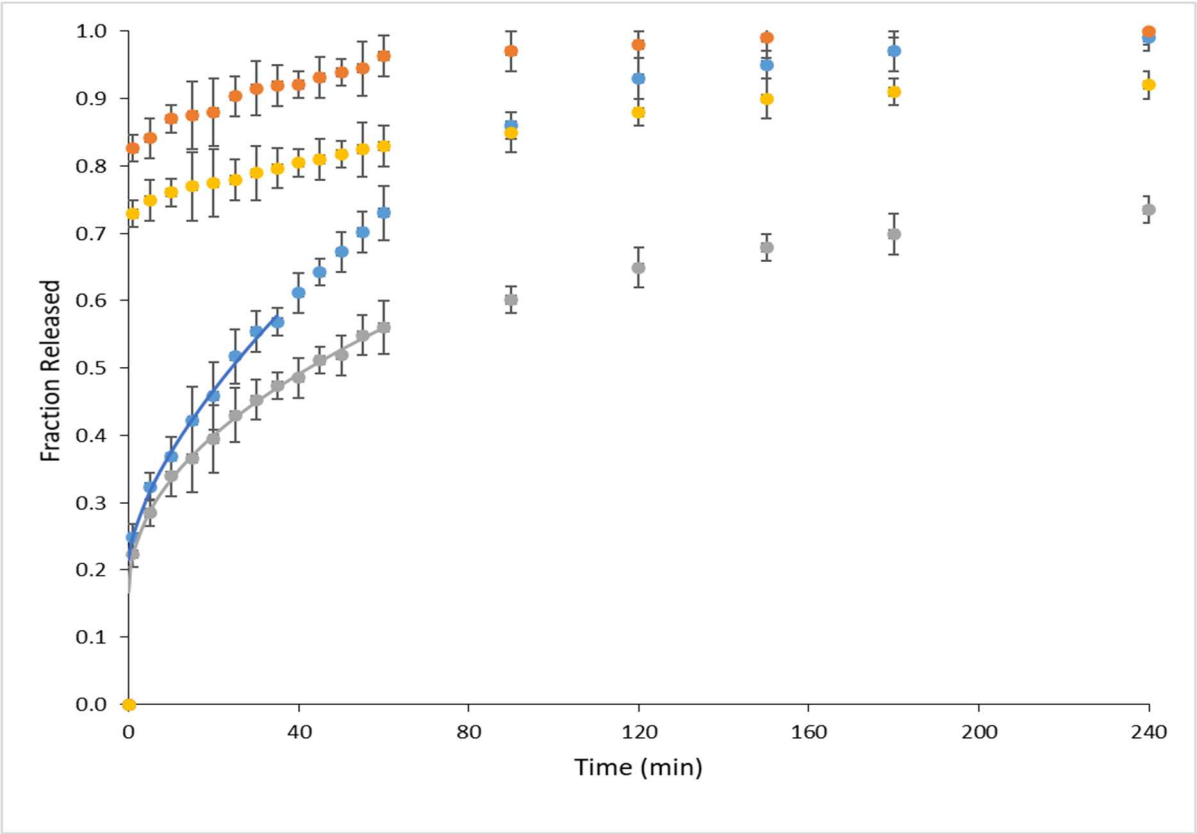

Fig. 4. Calculated fraction release of 5'-AMP in lactate buffer (5 mM, pH = 5) by SHMIP at 25°C (blue circle filled), SHMIP at 35°C (grey circle filled), SHNIP at 25°C (orange circle filled) and SHNIP at 35°C (yellow circle filled). Curves in blue and grey are based on theoretical values obtained by Korsmeyer-Peppas model (KP) for fractional release values ≤ 0.6 for SHMIP at 25°C and 35°C, respectively.

The obtained release kinetics are modelled in order to investigate the release mechanism and the effect of temperature. To this aim, several mathematical models have been selected as summarized in the Table S3. These models were chosen because they are the most used in the release studies, like the model of Baker and Lonsdale, developed in 1974, from the model described by Higuchi, for spherical matrices [56], or the Korsmeyer and Peppas model that described the release of a drug from hydrophilic polymers where the value of exponent *n*, characterizing the mechanism of release of drug, is given in the Table S3 [57]. Finally, the Fig. 4, where the ratio of quantity of 5'-AMP released on quantity of 5'-AMP initially

adsorbed onto the polymer, or $M_t/M\infty$, is plotted according time, showed three particular domains on the curves. The first domain was less than one minute, almost instantaneous, not negligible for SHMIP, where a majority of adsorbed 5'-AMP was released in the aqueous solution, and could be assimilate to a burst effect. So, both models retained and defined in Table S3, were implemented with the term *b*, which accounts for the burst term. This fact has been already demonstrated by Huang and Brazel [59], when they added to the "Korsmeyer and Peppas model" a constant to fit experimental data, accounting for a rapid jump in concentration at t=0. This term *b* was determined by extrapolation of release data to the start of the experiment.

Table 2. Estimated parameters obtained from fitting drug release data to Korsmeyer-Peppas and Baker-Lonsdale equations. The parameters are extracted of non-linear regression made on the first 60% of the release [58]. Grey cases showed the best model.

MIP 2		Baker-Lonsdale	Korsmeyer-Peppas
35°C	k	0.0051	0.05652
	n	/	0.47324
	b	0.0634	0.16709
	r^2	0.99034	0.99762
	χ^2	3.62×10^{-3}	2.53×10^{-5}
	F	2242	75447
25°C	k	0.00919	0.03568
	n	/	0.65244
	b	0.05784	0.21521
	r^2	0.99093	0.99227
	χ^2	1.32×10^{-3}	4.99×10^{-5}
	F	1327	25737

The choice of the best-fitting model is based on the value of *R* square (r^2), reduced chi square (χ^2) and Fisher test value (*F*), obtained by plotting the experimental results according to the

equations corresponding to the models studied. The closer to 1 the value of r^2 and smaller the values of χ^2 and F, better the model adjusts the data. The statistical values obtained for all the models are collected in the Table 2, as well as equation parameters. The more appropriate model, given by best-fitting statistical parameters, was the "Korsmeyer-Peppas" model where fractional release, defined by the amount of 5'-AMP released at time "t" (Mt) divided by amount of 5'-AMP loaded in SHMIP (M_∞), was a power function of time (see Table S3). The constant k was related to the rate of release, the exponent n was the diffusion exponent dependent on the release mechanism nature, and b was the parameter which represented the initial burst. In our case, for polymeric spheres, if the diffusion exponent was in the range of $0.43 < n < 0.85$, it indicated anomalous diffusion, i.e. non-Fickian diffusion. In this case, the release of drug was controlled by diffusion and polymer relaxation, such as swelling. A value of $n = 0.43$ indicated that only Fickian diffusion played a role in release process. And, a value of $n = 0.85$ indicated that change of the particles' size, or expansion of polymer, was the mean mechanism for drug release [60].

The imprinted hydrogel synthesized by inverse Pickering emulsion, SHMIP, showed a release profile very different from the non-imprinted one. First, the proportion of 5'-AMP released quasi- instantly after the contact of aqueous solution with polymers was higher for SHNIP than SHMIP. Practically 80% of the 5'-AMP was released from SHNIP, whatever the temperature, in less than one minute. While, for SHMIP, this phenomenon was close to 20%, only. When the percentages are translated in quantities, the amounts of 5'-AMP released by NIP and MIP during the burst domain were very close. This demonstrated that the burst phenomenon seen on these two polymers was due to the release of the bioactive adsorbed on surface by non-specific interactions. The 5'-AMP could easily be released from SHNIP matrix. But, SHMIP possessed selective binding cavities distributed throughout the surface and inside of the beads. And, this retention phenomenon of 5'-AMP in imprinted cavities

played a critical role in its release kinetics. It is showed that 5'-AMP is released according to diffusion phenomena due to an increasing concentration gradient of bioactive, but also to the swelling of the polymer. In fact, the exponent values were approximately 0.47 and 0.65 for SHMIP at 35°C and 25°C, respectively. These values were higher than 0.43, the limit exponent which shared the Fickian mechanism from non-Fickian one. At 25°C, the swelling of polymer and the diffusion explained the profile of release, with a first phenomenon maybe more present than diffusion, because the *n* value was higher than 0.43. But, at 35°C, it seemed that both processes of diffusion and relaxation had comparable rates. In this case, the relaxation became less important, thanks to the presence of NIPAM. This monomer allowed creating temperature-responsive polymer exhibiting a change in polymer conformation upon varying the temperature above Lower Critical Solution Temperature (LCST), admitted to be 32°C [61]. However, it has been previously demonstrated that the introduction of hydrophilic amine-containing monomers to NIPAM-based MIP hydrogels may lead to a significant broadening of the endothermal transitions associated with an increase in the LCST [62].

Herein, the investigation was performed at a simulated environmental skin temperature of 35°C, so that direct correlation between the thermal and release properties of SHMIP is rather difficult. However, we may assume that upon increasing the temperature above 32°C, SHMIP undergo a change in polarity, from hydrophilic to hydrophobic, associated with a shrinkage of hydrogel MIP in aqueous solution. Accordingly, the amount of polar 5'-AMP molecule released in solution increased more slowly as compared to what was observed at 25°C. This effect may be rationalized by the shrinking of the MIP matrix at 35°C hampering the release process and demonstrates the key role of temperature in the release of 5'-AMP from poly(NIPAM) imprinted polymeric spheres. These release data confirm that the molecularly imprinted hydrogel beads prepared by inverse Pickering emulsion polymerization provided a sustained release of 5'-AMP, in contrast to the corresponding non-imprinted hydrogel beads.

At a temperature of 35°C, 70% of the total amount of 5'-AMP loaded within the SHMIP (around 221 $mg.g^{-1}$) was released in lactic acid solution within 240 min, , while for the SHNIP, a fast release profile was observed as 80% of the total amount of in-MIP loaded 5'-AMP (53 $mg.g^{-1}$) was released within

Conclusions

This work reports for the first time the design and synthesis of a molecularly imprinted hydrogel selective to the nucleotide adenosine 5′-monophosphate using inverse Pickering emulsion technology. The monomers used in the formulation of MIPs, namely 2-(dimethylamino)ethyl methacrylate and N-isopropylacrylamide, allowed stabilizing the pre-polymerization complex through electrostatic interactions, hydrogen bonding and hydrophobic interactions. The adsorption behaviour of the hydrogel MIP was thoroughly investigated and adsorption isotherms best-fitted the Hill model, suggesting the occurrence of a positive cooperativity phenomenon. As such, more than one molecule of 5'-AMP could be interacting by binding cavity in the MIP. The results also showed that the molecularly imprinted beads possessed a higher capacity and greater imprinting factor for 5'-AMP than non-imprinted ones. Release of the bioactive nucleotide adsorbed in the imprinted polymeric matrix seemed to follow three mechanisms, as demonstrated by the modified Korsmeyer-Peppas model. A weak burst effect played an immediate role providing desorption of 5'-AMP molecules retained on the polymers' surface by non-specific interactions. This finding explains why the burst effect was more pronounced with the NIP as compared to MIP. Upon polymer swelling, the disruption of selective interactions between 5'-AMP and polymer occurred and finally, the release of 5'-AMP in the aqueous medium is controlled by a simple diffusion phenomena. Effect of temperature on the release profile was also investigated. The

temperature decreased the rate of 5'-AMP release because the conformation of the polymer changed, and at 35°C the polymer relaxation coefficient was low. So, the newly developed MIP allowed sustained release of 5'-AMP within 4 hours demonstrating the potential of hydrogel MIPs as topical drug delivery systems for cosmetology.

Acknowledgements

This work was funded by Region Centre - Val de Loire, by the Cosme-MIP and Cargo-Ther projects. M.G. Ayari and P. Kadhirvel thank Region Centre - Val de Loire for the PhD and post-doctoral fellowships, respectively.

References

[1] B. Sellergren, A.J. Hall, In Techniques and Instrumentation in Analytical Chemistry, 1st ed.; Sellergren, B.S., Ed.; Elsevier Science: 2000; Chapter 2, Fundamental aspects on the synthesis and characterization of imprinted network polymers, Vol. 23, pp. 21-57.

[2] A.G. Mayes, M.J. Whitcombe, Synthetic strategies for the generation of molecularly imprinted organic polymers, Advanced Drug Delivery Reviews 57 (2005) 1742-1778.

[3] M.J. Whitcombe, L. Martin, E.N. Vulfson, Predicting the selectivity of imprinted polymers, Chromatographia 47 (1998) 457-464.

[4] X. Song, J. Wang, J. Zhu, Effect of porogenic solvent on selective performance of molecularly imprinted polymer for quercetin, Materials Research 12 (2009) 299-304.

[5] K. Karim, F. Breton, R. Rouillon, E.V. Piletska, A. Guerreiro, I. Chianella, S.A. Piletsky, How to find effective functional monomers for effective molecularly imprinted polymers? Advanced Drug Delivery Reviews 57 (2005) 1795-808.

[6] T. Muhammad, Z. Nur, E.V. Piletska, O. Yimit, S.A. Piletsky, Rational design of molecularly imprinted polymer: the choice of cross-linker, Analyst 137 (2012) 2623-2628.

[7] I. Mijangos, F. Navarro-Villoslada, A. Guerreiro, E. Piletska, I. Chianella, K. Karim, A. Turner, S. Piletsky, Influence of initiator and different polymerisation conditions on performance of molecularly imprinted polymers, Biosensors and Bioelectronics 22 (2006) 381-387.

[8] K. Karim, T. Cowen, A. Guerreiro, E. Piletska, M.J. Whitcombe, S.A. Piletsky, A Protocol for the Computational Design of High Affinity Molecularly Imprinted Polymer Synthetic Receptors, Global Journal of Biotechnology and Biomaterial Science 3 (2017) 1-7.

[9] G. Wulff, B.O. Chong, U. Kolb, Soluble single-molecule nanogels of controlled structure as a matrix for efficient artificial enzymes, Angewandte Chemie International Edition 45 (2006) 2955-2958.

[10] P. Çakir, A. Cutivet, M. Resmini, B. Tse Sum Bui, K. Haupt, Protein-Size Molecularly Imprinted Polymer Nanogels as Synthetic Antibodies, by Localized Polymerization with Multi-initiators, Advanced Materials 25 (2013) 1048-1051.

[11] K. Smolinska-Kempisty, A. Guerreiro, F. Canfarotta, C. Cáceres, M.J. Whitcombe, S.A. Piletsky, A comparison of the performance of molecularly imprinted polymer nanoparticles for small molecule targets and antibodies in the ELISA format, Scientific Reports 6 (2016) 37638.

[12] D. Cunliffe, A. Kirby, A. Alexander, Molecularly imprinted drug delivery systems, Advanced Drug Delivery Reviews 57 (2005) 1836-1853.

[13] C. Alvarez-Lorenzo, A. Concheiro, Molecularly imprinted polymers for drug delivery, Journal of Chromatography B 804 (2004) 231-245.

[14] S.A. Zaidi, Latest trends in molecular imprinted polymer based drug delivery systems, RSC Advances 6 (2016) 88807–88819.

[15] M. Ali, M.E. Byrne, Controlled Release of High Molecular Weight Hyaluronic Acid from Molecularly Imprinted Hydrogel Contact Lenses, Pharmaceutical Research 26 (2009) 714-726.

[16] Delivery System Handbook for Personal Care and Cosmetic Products-Technology, Applications, and Formulations, 1st ed.; M.R. Rosen; Ed.; William Andrew: New-York, 2005.

[17] R. Ganceviciene, A.I. Liakou, A. Theodoridis, E. Makrantonaki, C.C. Zouboulis, Skin anti-aging strategies, Dermato-Endocrinology 4 (2012) 308–319.

[18] F. Furukawa, S. Kanehara, F. Harano, S. Shinohara, J. Kamimura, S. Kawabata, S. Igarashi, M. Kawamura, Y. Yamamoto, Y. Miyachi, Effects of adenosine 5'-monophosphate on epidermal turnover, Archives of Dermatological Research 300 (2008) 485–493.

[19] B. Sellergren, J. Wieschemeyer, K.S. Boos, D. Seidel, Imprinted Polymers for Selective Adsorption of Cholesterol from Gastrointestinal Fluids, Chemistry of Materials 10 (1998) 4037-4046.

[20] J.G. Karlsson, L.I. Andersson, I.A. Nicholls, Probing the molecular basis for ligand-selective recognition in molecularly imprinted polymers selective for the local anaesthetic bupivacaine, Analytica Chimica Acta 435 (2001) 57-64.

[21] Y. Kanekiyo, Y. Ono, K. Inoue, M. Sano, S. Shinkai, 'Molecular-imprinting' in polyion complexes which creates the 'memory' for the AMP template, Journal of the Chemical Society Perkin Transactions 2 0 (1999) 557–561

[22] Y. Kanekiyo, K. Inoue, Y. Ono, M. Sano, S. Shinkai, D.N. Reinhoudt, 'Molecular-imprinting' of AMP utilising the polyion complex formation process as detected by a QCM system, Journal of the Chemical Society Perkin Transactions 2 0 (1999) 2719–2722

[23] Y. Kanekiyo, M. Sano, R. Iguchi, S. Shinkai, Novel Nucleotide-Responsive Hydrogels Designed from Copolymers of Boronic Acid and Cationic Units and Their Applications as a QCM Resonator System to Nucleotide Sensing, Journal of Polymer Science: Part A: Polymer Chemistry 38 (2000) 1302–1310.

[24] B. Dirion, Z. Cobb, E. Schillinger, L.I. Andersson, B. Sellergren, Water-Compatible Molecularly Imprinted Polymers Obtained via High-Throughput Synthesis and Experimental Design, Journal of the American Chemical Society 125 (2003) 15101–15109.

[25] X. Shen, L. Ye, Molecular imprinting in Pickering emulsions: a new insight into molecular recognition in water, Chemical Communications 47 (2011) 10359–10361.

[26] X. Shen, T. Zhou, L. Ye, Molecular imprinting of protein in Pickering emulsion, Chemical Communications 48 (2012) 8198–8200.

[27] F. Breton, R. Delépée, L.A. Agrofoglio, Molecular imprinting of AMP by an ionic-noncovalent dual approach, Journal of Separation Science 32 (2009) 3285-3291.

[28] F. Breton, R. Delépée, D. Jégourel, D. Deville-Bonne, L.A. Agrofoglio, Selective adenosine-5'-monophosphate uptake by water-compatible molecularly imprinted polymer, Analytica Chimica Acta 616 (2008) 222-229.

[29] L. Qin, X.W. He, W.Y. Li, Y.K. Zhang, Molecularly imprinted polymer prepared with bonded beta-cyclodextrin and acrylamide on functionalized silica gel for selective recognition of tryptophan in aqueous media, Journal of Chromatography A 1187 (2008) 94–102.

[30] L. Duan, M. Chen, S. Zhou, L. Wu, Synthesis and Characterization of Poly[N-isopropylacrylamide]/Silica Compocavity Microspheres via Inverse Pickering Suspension Polymerization, Langmuir 25 (2009) 3467-3472.

[31] Z. Zhang, K.C. Tam, X. Wang, G. Sèbe, Inverse Pickering Emulsions Stabilized by Cinnamate Modified Cellulose Nanocrystals as Templates To Prepare Silica Colloidosomes, ACS Sustainable Chemistry and Engineering 6 (2018) 2583−2590

[32] J. Bai, Y. Zhang, L. Chen, H. Yan, C. Zhang, L. Liu, X. Xu, Synthesis and characterization of paclitaxel-imprinted microparticles for controlled release of an anticancer drug, Materials Science and Engineering: C, Materials for Biological Applications 92 (2018) 338-348

[33] F.J. Xu, H. Li, J. Li, Z. Zhang, E.T. Kang, K.G. Neoh, Pentablock copolymers of poly[ethylene glycol], poly [[2-dimethyl amino] ethyl methacrylate] and poly [2-hydroxethyl methacrylate] from consecutive atom transfer radical polymerizations for non-viral gene delivery, Biomaterials 19 (2008) 3023–3033.

[34] MarvinSketch, version 6.2.2, calculation module developed by ChemAxon, http://www.chemaxon.com/products/marvin/marvinsketch/, 2014

[35] M.A. Cooperstein, H.E. Canavan, Assessment of cytotoxicity of [N-isopropylacrylamide] and Poly[N-isopropyl acrylamide]-coated surfaces, Biointerphases 8 (2013) 19.

[36] J. Moselhy, S. Sarkar, M.C. Chia, J.D. Mocanu, N. Taulier, F.F. Liu, X.Y. Wu, Evaluation of copolymers of N-isopropylacrylamide and 2-dimethyl[aminoethyl]methacrylate in nonviral and adenoviral vectors for gene delivery to nasopharyngeal carcinoma, International Journal of Nanomedicine 2 (2007) 461–478.

[37] Biomedical Applications of Hydrogels Handbook, 1st Ed.; R.M. Ottenbrite, K. Park, T. Okano, Eds.; Springer-Verlag: New York, 2010.

[38] K. Koyanagi, Y. Takashima, T. Nakamura, H. Yamaguchi, A. Harada, Radical polymerization by a supramolecular catalyst: cyclodextrin with a RAFT reagent, Beilstein Journal of Organic Chemistry 12 (2016) 2495–2502.

[39] K. Zhang, W. Wu, H. Meng, K. Guo, J.F. Chen, Pickering emulsion polymerization: Preparation of polystyrene/nano-SiO_2 compocavity microspheres with core-shell structure, Powder Technology 190 (2009) 393–400.

[40] P. Finkle, H.D. Draper, J.H. Hildebrand, The theory of emulsification, Journal of the American Chemical Society 45 (1923) 2780-2788.

[41] B.P. Binks, S.O. Lumsdon, Effects of oil type and aqueous phase composition on oil water mixtures containing particles of intermediate hydrophobicity, Physical Chemistry Chemical Physics 2 (2000) 2959-2967.

[42] A.S. Kabalnov, A.V. Pertzov, E.D. Shchukin, Ostwald ripening in emulsions: I. Direct observations of Ostwald ripening in emulsions, Journal of Colloid and Interface Science 118 (1987) 590-597.

[43] T. Sharma, G.S. Kumar, B.H. Chon, J.S. Sangwai, Thermal stability of oil-in-water Pickering emulsion in the presence of nanoparticle, surfactant, and polymer, Journal of Industrial and Engineering Chemistry 22 (2015) 324–334.

[44] D. Spivak, M.A. Gilmore, K.J. Shea, Evaluation of binding and origins of specificity of 9-ethyladenine imprinted polymers, Journal of the American Chemical Society 119 (1997) 4388–4393.

[45] U. Athikomrattanakul, M. Katterle, N. Gajovic-Eichelmann, F.W. Scheller, Development of molecularly imprinted polymers for the binding of nitrofurantoin, Biosensors and Bioelectronics 25 (2009) 82–87.

[46] G. Vasapollo, R. Del Sole, L. Mergola, M.R. Lazzoi, A. Scardino, S. Scorrano, G. Mele, Molecularly Imprinted Polymers: Present and Future Prospective, International Journal of Molecular Sciences 12 (2011) 5908-5945.

[47] R.J. Umpleby, S.C. Baxter, Y. Chen, R.N. Shah, K.D. Shimizu, Characterization of molecularly imprinted polymers with the Langmuir-Freundlich isotherm, Analytical Chemistry 73 (2001) 4584-4591.

[48] L.K. Koopal, W.H. van Riemsdijk, J.C.M. de Witt, M.F. Benedetti, Analytical isotherm equations for multicomponent adsorption to heterogeneous surfaces, Journal of Colloid and Interface Science 166 (1994) 51-60.

[49] N. Lavignac, K.R. Brain, C.J. Allender, Concentration dependent atrazine–atrazine complex formation promotes selectivity in atrazine imprinted polymers, Biosensors and Bioelectronics 22 (2006) 138–144.

[50] M.C. Ncibi, Applicability of some statistical tools to predict optimum adsorption isotherm after linear and non-linear regression analysis, Journal of Hazardous Materials 153 (2008) 207–212.

[51] J.A. Garcia-Calzon, M.E. Diaz-Garcia, Characterization of binding cavities in molecularly imprinted polymers, Sensors and Actuators B: Chemical 123 (2007) 1180–1194.

[52] P. Kadhirvel, M. Azenha, S. Shinde, E. Schillinger, P. Gomes, B. Sellergren, A.F. Silva, Imidazolium-based functional monomers for the imprinting of the anti-inflammatory drug naproxen: Comparison of acrylic and sol–gel approaches, Journal of Chromatography A 1314 (2013) 115-123.

[53] B. Li, J. Xu, A. Hall, K. Haupt, B. Tse Sum Bui, Water-compatible silica sol-gel molecularly imprinted polymer as a potential delivery system for the controlled release of salicylic acid, Journal of Molecular Recognition 27 (2014) 559-565.

[54] V.D. Salian, M.E. Byrne, Controlled Drug Release from Weakly Crosslinked Molecularly Imprinted Networks: The Benefit of Living Radical Polymerization, Macromolecular Chemistry and Physics 214 (2013) 2355−2366.

[55] H. Lambers, S. Piessens, A. Bloem, H. Pronk, P. Finkel, Natural skin surface pH is on average below 5, which is beneficial for its resident flora, International Journal of Cosmetic Science 28 (2006) 359-370.

[56] R.W. Baker, H.S. Lonsdale, Controlled release: mechanisms and rates. In Controlled Release of Biologically Active Agents, 1st ed.; A.C. Tanquary, R.E Lacey, Eds.; Plenum Press: New York, 1974, 15-71.

[57] R.W. Korsmeyer, R. Gurny, E. Doelker, P. Buri, N.A. Peppas, Mechanisms of solute release from porous hydrophilic polymers, International Journal of Pharmaceutics 15 (1983) 25–35.

[58] X. Huang, C.S. Brazel, On the importance and mechanisms of burst release in matrix-controlled drug delivery systems, Journal of Controlled Release 73 (2001) 121–136.

[59] J. Siepmann, F. Siepmann, Modeling of diffusion controlled drug delivery, Journal of Controlled Release 161 (2012) 351-362.

[60] P. Ritger, N. Peppas, A simple equation for description of solute release. II. Fickian and anomalous release from swellable devices, Journal of Controlled Release 5 (1987) 37-42.

[61] A. Gandhi, A. Paul, S.O. Sen, K.K. Sen, Studies on thermoresponsive polymers: Phase behaviour, drug delivery and biomedical applications, Asian Journal of Pharmaceutical Sciences 10 (2015) 99-107.

[62] Z.D. Hua, Z.Y. Chen, Y.Z. Li, M.P. Zhao, Thermosensitive and Salt-Sensitive Molecularly Imprinted Hydrogel for Bovine Serum Albumin, Langmuir 24 (2008) 5773-5780

[1] Both authors have contributed equally to this work.